CORRIGENDUM

A serine-substituted P450 catalyzes highly efficient carbene transfer to olefins *in vivo*

Pedro S Coelho, Z Jane Wang, Maraia E Ener, Stefanie A Baril, Arvind Kannan, Frances H Arnold & Eric M Brustad

Nat. Chem. Biol. **9**, 485–487 (2013); published online 23 June 2013; corrected after print 19 December 2013

In the version of this article initially published, the Protein Data Bank codes for the P450 and P411 constructs were inadvertently switched. Accession code 4H23 actually corresponds to the P411 structure, and 4H24 corresponds to the P450 structure. The error has been corrected in the HTML and PDF versions of the article.

CORRECTION NOTICE

Nat. Chem. Biol. **9**, 485–487 (2013)

A serine-substituted P450 catalyzes highly efficient carbene transfer to olefins *in vivo*

Pedro S Coelho, Z Jane Wang, Maraia E Ener, Stefanie A Baril, Arvind Kannan, Frances H Arnold & Eric M Brustad

In the version of this supplementary file originally posted online, the axes, and in one case, data, for the graphs shown in Supplementary Figures 2, 16 and 17 were inadvertently lost. The full graphs are now provided as of 18 July 2013.

Supplementary Results for

A Serine-Substituted P450 Catalyzes Highly Efficient Carbene Transfer to Olefins *In Vivo*

Pedro S. Coelho[1], Z. Jane Wang[1], Maraia E. Ener[1], Stefanie A. Baril[2], Arvind Kannan[1],

Frances H. Arnold[1]*, Eric M. Brustad[2,3]*

Affiliations:

[1] Division of Chemistry and Chemical Engineering, California Institute of Technology, Pasadena, CA 91125, USA.
[2]Department of Chemistry, University of North Carolina at Chapel Hill, Chapel Hill, NC 27599, USA.
[3] Carolina Center for Genome Sciences, University of North Carolina at Chapel Hill, Chapel Hill, NC 27599, USA.

* Correspondence to: frances@cheme.caltech.edu, brustad@email.unc.edu

Nature Chemical Biology: doi:10.1038/nchembio.1278

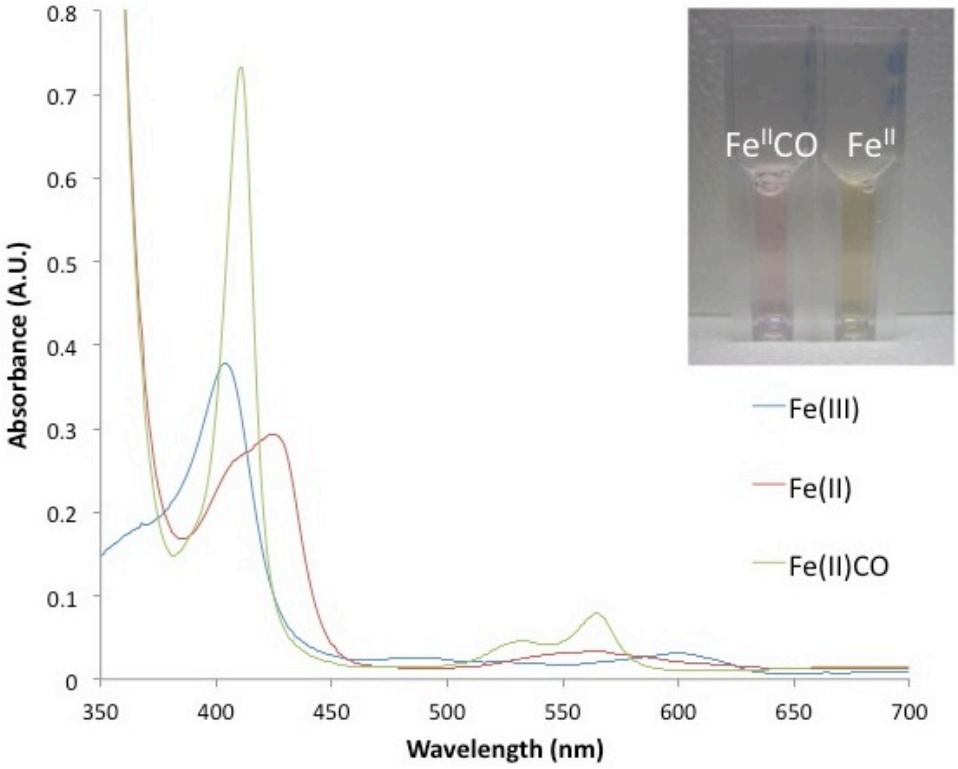

Supplementary Figure 1: Electronic absorption spectra for ferric (blue), dithionite-reduced ferrous (red) and carbon monoxide-bound ferrous (green) $P411_{BM3\text{-}heme}$-CIS. Soret bands (nm): Fe^{III}, 404; Fe^{II}, 410, 425; Fe^{II}-CO, 411. Fe^{II}-CO displays α and β bands at 532 and 565 nm. Insert shows the carbon monoxide ferrous (pink) and the dithionite-reduced ferrous (yellow) enzymes at 4.5 μM protein concentration. The shoulder at 410 nm for the ferrous spectrum is due to incomplete reduction to Fe^{II} under the aerobic conditions in which these spectra were taken. Reduction of cytochrome P411 under strict anaerobic conditions, as is the case for the redox titrations (**Supplementary Figs. 7** and **9**), gives a single peak at 421 nm.

Nature Chemical Biology: doi:10.1038/nchembio.1278

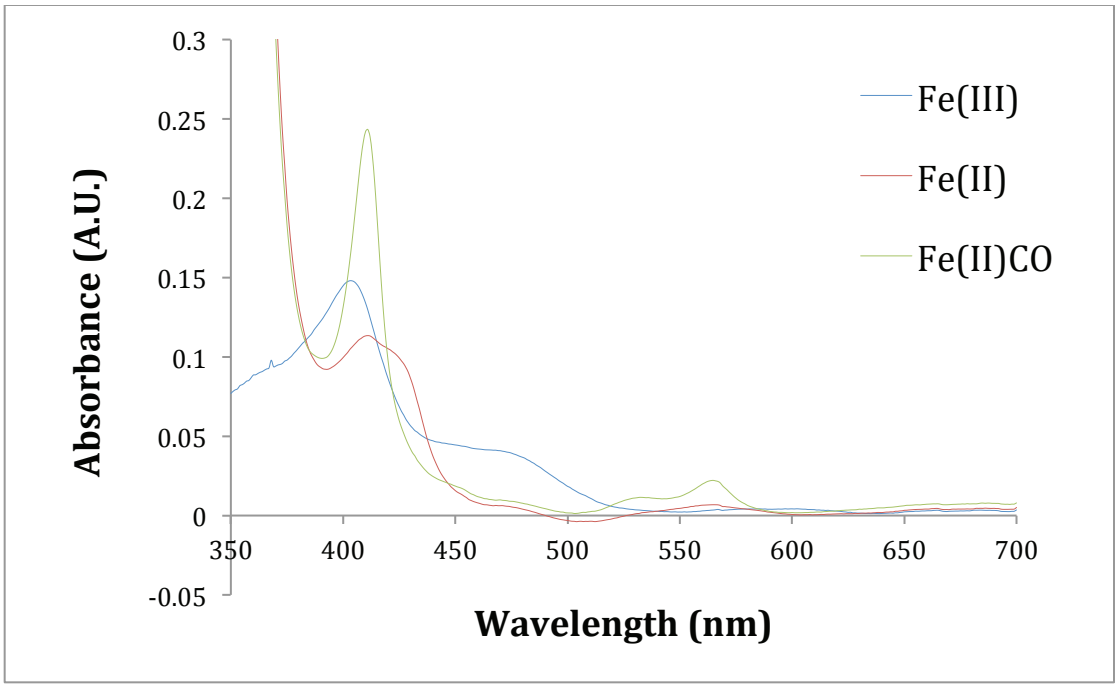

Supplementary Figure 2: Electronic absorption spectra for ferric (blue), dithionite-reduced ferrous (red) and carbon monoxide-bound ferrous (green) full-length $P411_{BM3}$-CIS. Soret bands (nm): Fe^{III}, 404; Fe^{II}, 410, 422; Fe^{II}-CO, 411. Fe^{II}-CO displays α and β bands at 533 and 566 nm. Ferric spectrum displays a broad peak at 465 nm.

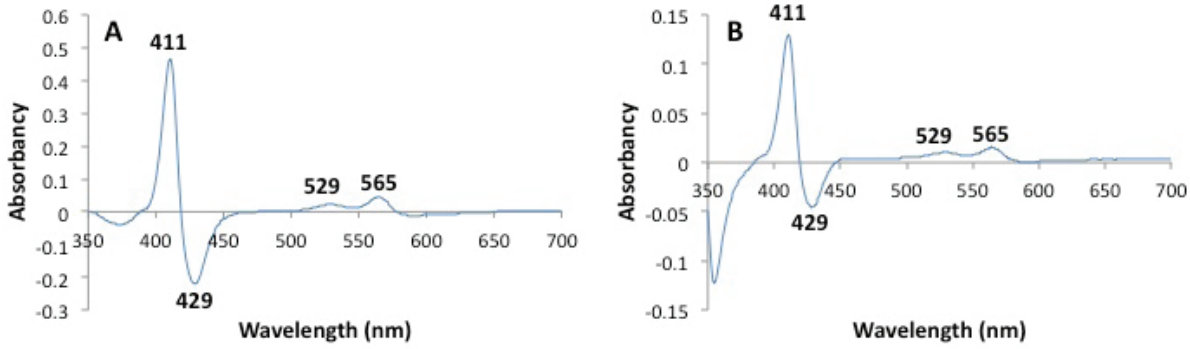

Supplementary Figure 3: Difference spectra for ferrous carbonyl with respect to ferrous for: (**A**) $P411_{BM3\text{-}heme}$-CIS and (**B**) $P411_{BM3}$-CIS.

Supplementary Table 1: Comparison of λmax for $P411_{BM3\text{-}heme}$-CIS and CYP2B4-C436S[1]

	$P411_{BM3\text{-}heme}$-CIS **(nm)**	**CYP2B4-C436S (nm)**
Ferric resting state	404	405
Ferrous	425	422
Ferrous-CO	411	413

Nature Chemical Biology: doi:10.1038/nchembio.1278

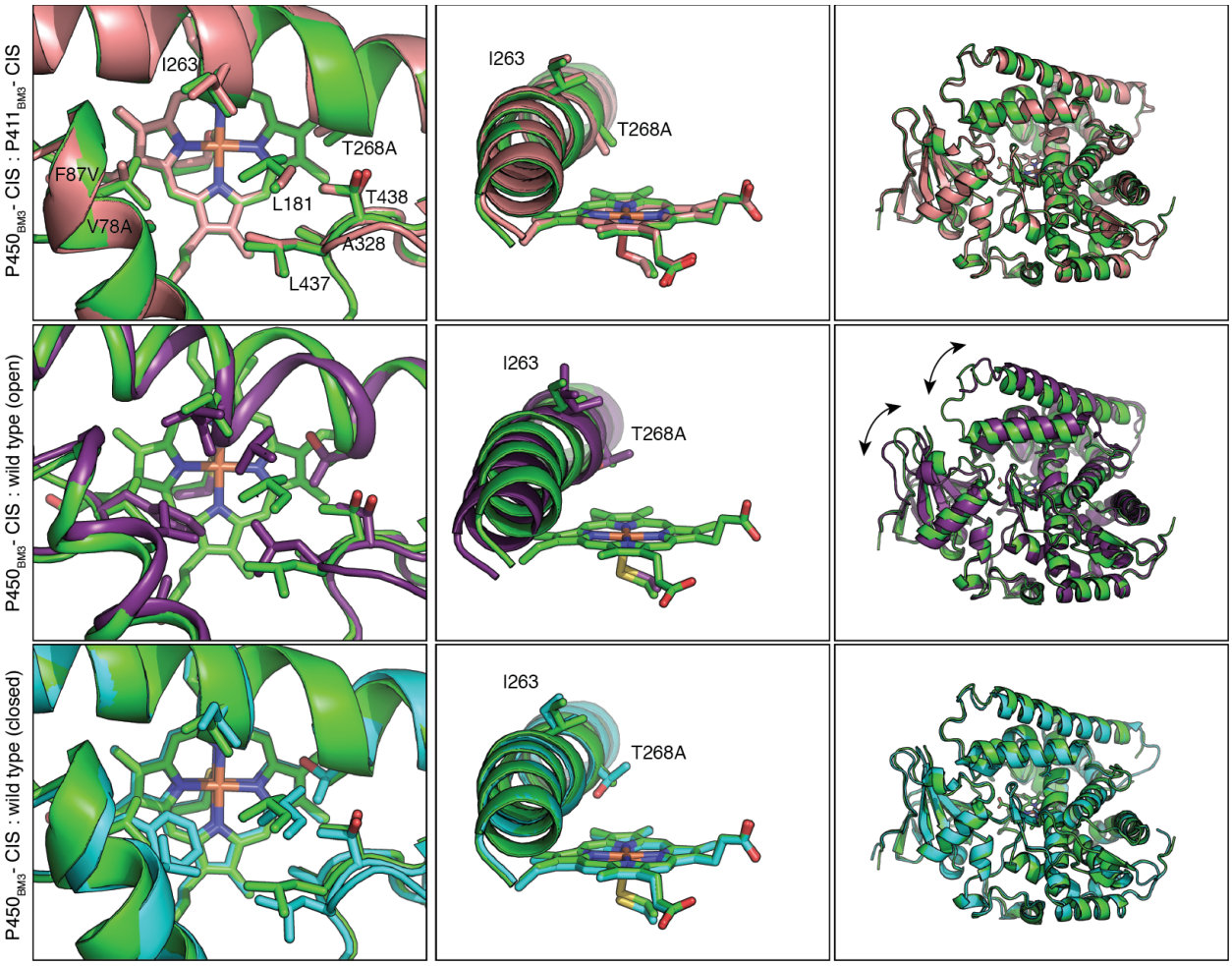

Supplementary Figure 4: Heme domain active site and protein alignments of $P450_{BM3}$-CIS with $P411_{BM3}$-CIS and wild type $P450_{BM3}$. Top panels shows alignments of $P450_{BM3}$-CIS (green) and $P411_{BM3}$-CIS (peach) with left, middle and right panels showing active site residues, the active site I-helix, and global protein fold, respectively. No significant structural changes were observed (RMSD 0.52 Å). Middle panels: Large variations are observed upon comparing $P411_{BM3}$-CIS with the open (ligand-free) form of wild type $P450_{BM3}$ (purple, taken from PDB# 2IJ2, RMSD 1.2 Å). Pronounced rearrangements are observed in active site side chain residues (left) as well as rotations within the I-helix. Global movements are also observed in the N-terminal beta domain as well as F- and G- helices (right, marked by double headed arrows). These movements are consistent with well-known transitions that occur upon substrate binding and are important for native monooxygenation catalysis. Bottom panels: Alignment of $P450_{BM3}$-CIS with a ligand-bound $P450_{BM3}$ structure (cyan, taken from PDB# 1JPZ, RMSD 0.52 Å) demonstrates that $P450_{BM3}$-CIS and $P411_{BM3}$-CIS mimic the closed protein conformation even in the absence of substrate. Protein alignments were carried out using the align tool of PyMol (PyMOL Molecular Graphics System, Version 1.3 Schrödinger, LLC.).

Nature Chemical Biology: doi:10.1038/nchembio.1278

Supplementary Table 2. Data collection and refinement statistics for cytochrome P450 and P411 crystals.

	$P450_{BM3\text{-}heme}$-CIS	$P411_{BM3\text{-}heme}$-CIS
pdb accession #	**4H24**	**4H23**
Data collection*		
Space group	I 1 2 1	P 2 21 21
wavelength	1.033	1.033
Cell dimensions		
a, *b*, *c* (Å)	187.79, 62.74, 210.28	63.16, 124.46, 127.69
α, β, γ (°)	90.00, 115.75, 90.00	90.00, 90.00, 90.00
Resolution (Å)	48.6 - 2.5 (2.5 - 2.6) **	44.9 – 3.3 (3.3 – 3.5) **
R_{merge}	5.3(39.5)	17.6(51.4)
$I / \sigma I$	13.4(3.0)	11.8(5.7)
Completeness (%)	98.7(99.2)	99.9(99.9)
Redundancy	2.6(2.6)	5.3(5.4)
Refinement		
Resolution (Å)	48.6 - 2.5	44.9 – 3.3
No. reflections	72085	14884
R_{work} / R_{free}	0.19 / 0.25	0.18/0.26
No. atoms		
Protein	14401	6890
Ligand/ion	128	86
Water	196	24
B-factors		
Protein	33.9	25.4
Ligand/ion	25.4	19.9
Water	26.7	18.9
R.m.s. deviations		
Bond lengths (Å)	0.017	0.016
Bond angles (°)	1.70	1.65
Ramachandran outliers***	0.3 %	0.7 %

*All data sets were collected from single crystals.
**Highest-resolution shell is shown in parentheses.
*** Ramachandran outliers lie in regions of protein that are known to be flexible and show similar disorder among $P450_{BM3}$ structures in the literature.

Nature Chemical Biology: doi:10.1038/nchembio.1278

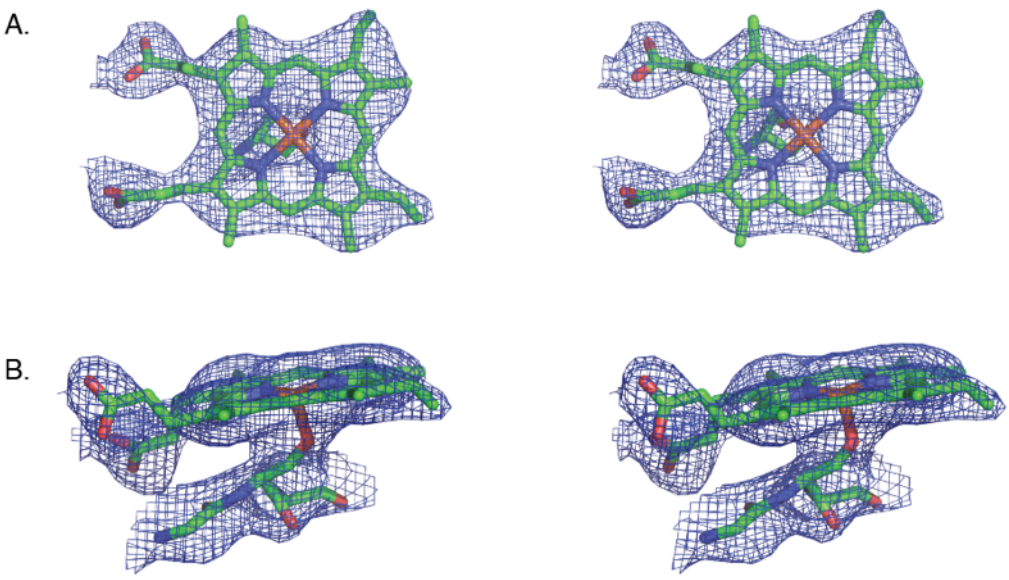

Supplementary Figure 5: Heme electron density of $P411_{BM3}$-CIS. Maximum likelihood weighted electron density maps of serine-ligated heme in $P411_{BM3}$-CIS. (A) Stereo image of heme bound to $P411_{BM3}$-CIS viewed from the top of the heme in the active site. (B) Stereo image of heme bound to $P411_{BM3}$-CIS rotated ~ 90° from panel A shows clear indication of heme-iron ligation by the side chain hydroxyl of C400S. All atoms are shown as sticks. All electron density maps were contoured at $\sigma = 1.0$. For perspective, in panel B, the main chain atoms of residues 399 and 401 are also shown as sticks.

Nature Chemical Biology: doi:10.1038/nchembio.1278

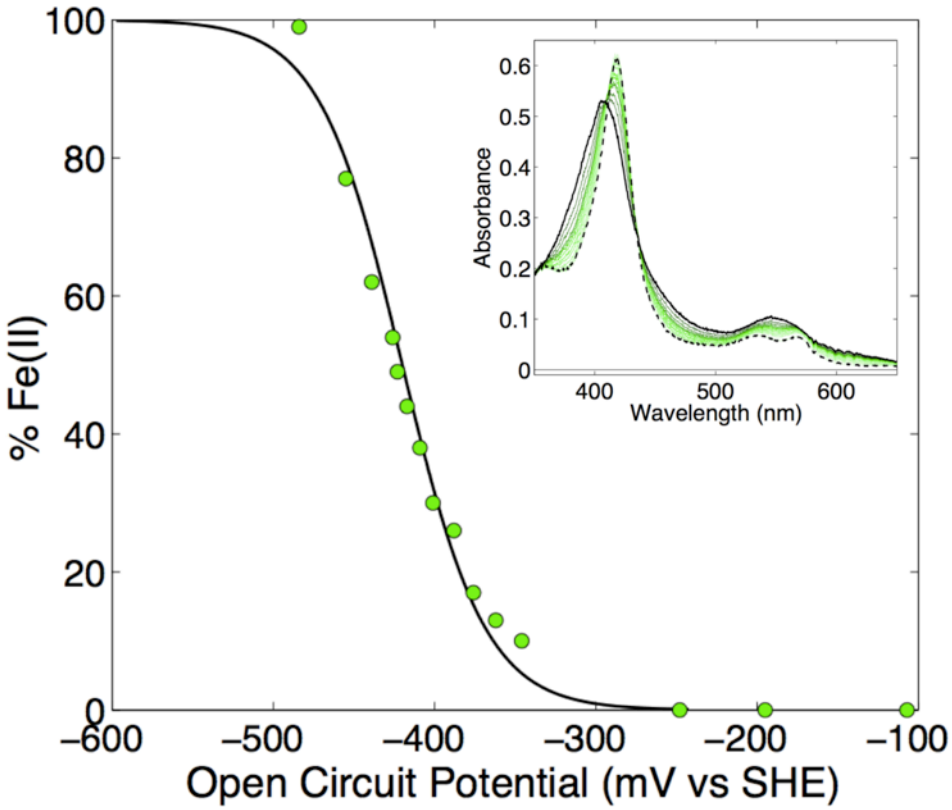

Supplementary Figure 6: Potentiometric redox titration for $P450_{BM3\text{-}heme}$ with overlaid Nernst curve fit to $E°' = -420$ mV. Inset shows spectral changes upon each sub-stoichiometric addition of sodium dithionite (dashed line: fully ferric; solid line: fully ferrous). See **Online Methods** for detailed error analysis.

Nature Chemical Biology: doi:10.1038/nchembio.1278

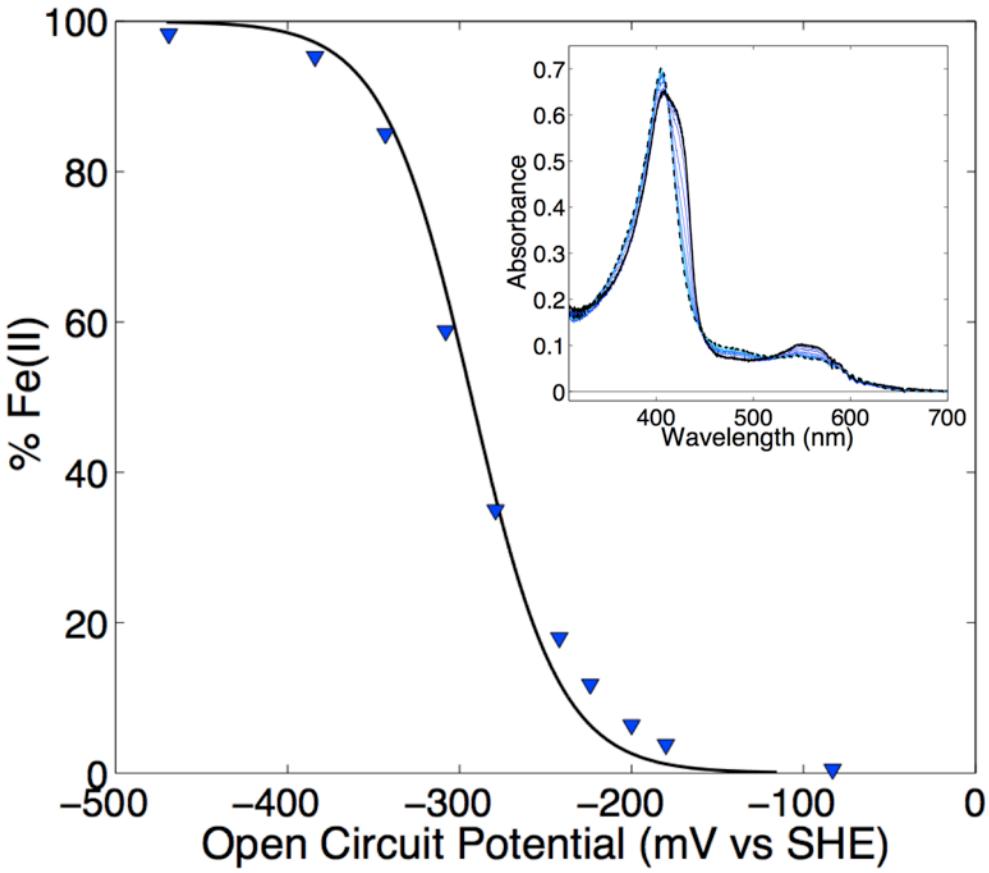

Supplementary Figure 7: Potentiometric redox titration for $P411_{BM3\text{-}heme}$ with overlaid Nernst curve fit to $E°' = -293$ mV. Inset shows spectral changes upon each sub-stoichiometric addition of sodium dithionite (dashed line: fully ferric; solid line: fully ferrous). See **Online Methods** for detailed error analysis.

Nature Chemical Biology: doi:10.1038/nchembio.1278

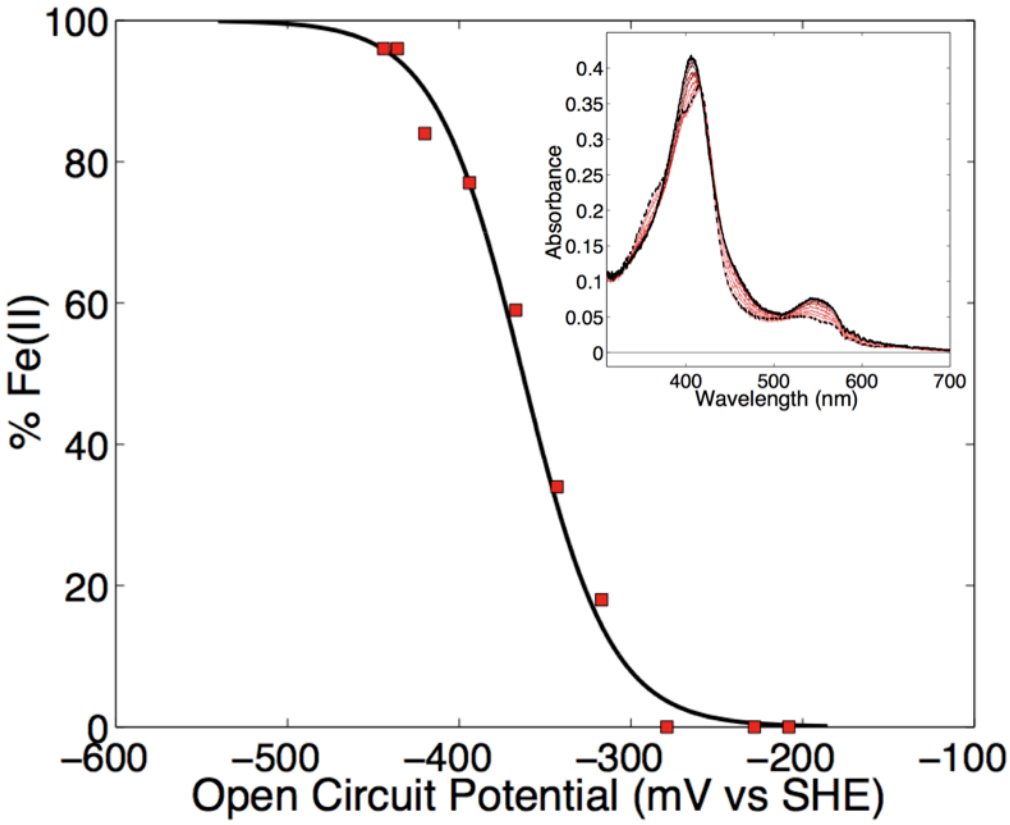

Supplementary Figure 8: Potentiometric redox titration for $P450_{BM3\text{-}heme}$-CIS with overlaid Nernst curve fit to $E°' = -360$ mV. Inset shows spectral changes upon each sub-stoichiometric addition of sodium dithionite (dashed line: fully ferric; solid line: fully ferrous). See **Online Methods** for detailed error analysis.

Nature Chemical Biology: doi:10.1038/nchembio.1278

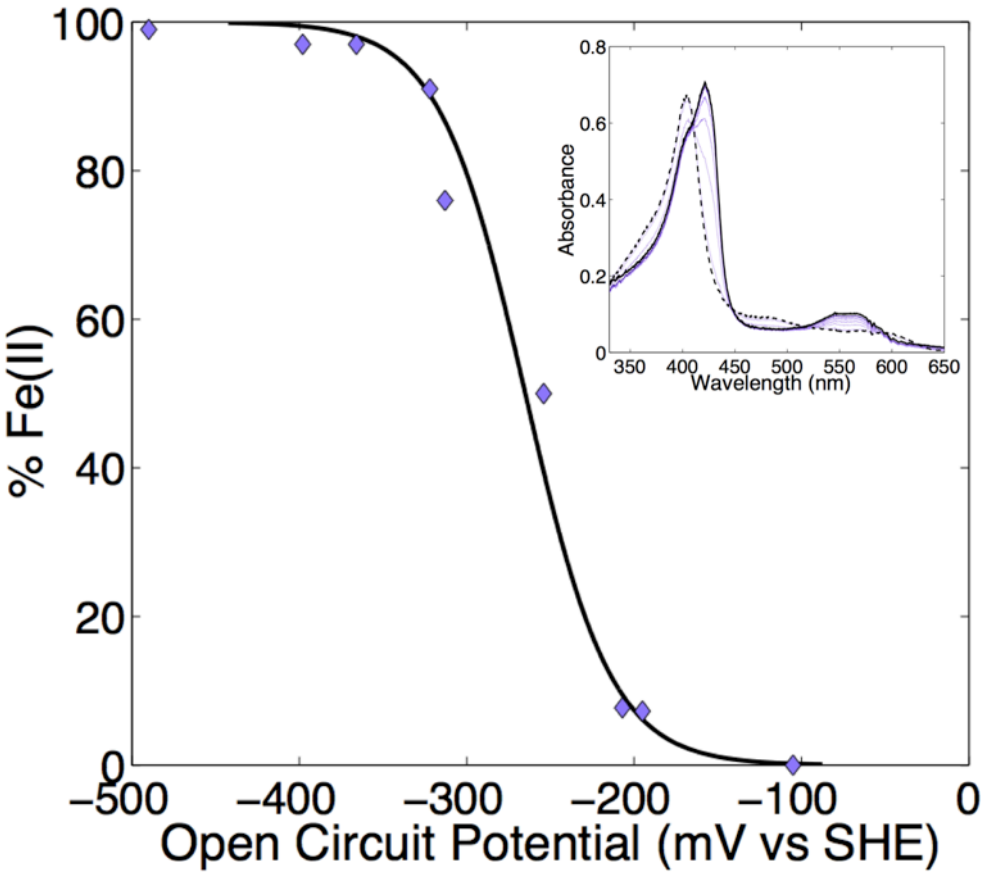

Supplementary Figure 9: Potentiometric redox titration for $P411_{BM3\text{-}heme}$-CIS with overlaid Nernst curve fit to $E°' = -265$ mV. Inset shows spectral changes upon each sub-stoichiometric addition of sodium dithionite (dashed line: fully ferric; solid line: fully ferrous). See **Online Methods** for detailed error analysis.

Nature Chemical Biology: doi:10.1038/nchembio.1278

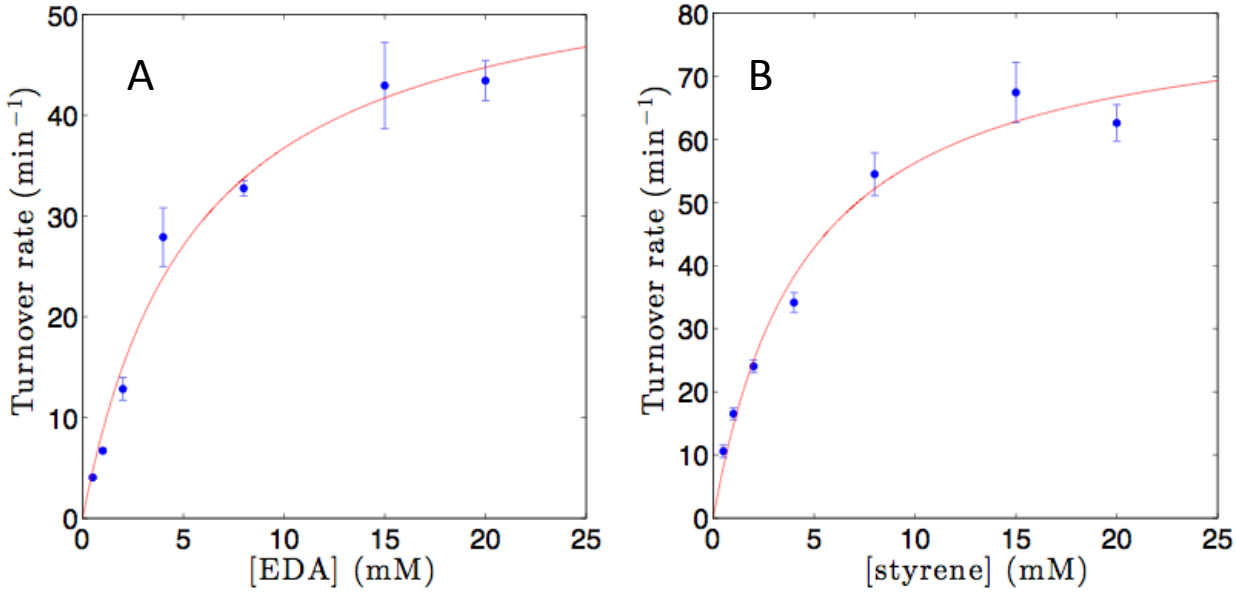

Supplementary Figure 10: Initial velocities plot for P411$_{BM3\text{-}heme}$-CIS. (**A**) EDA concentration was varied at a saturating concentration of styrene (30 mM). (**B**) Styrene concentration was varied at a fixed concentration of EDA (20 mM). Initial rates were computed as the slope of a zero-intercept linear fit of three different time points from independent reactions. Error bars correspond to 1-σ (68.3%) confidence intervals for the slope.

Supplementary Table 3: Michaelis-Menten parameters for P450 cyclopropanation catalysts. Error bars correspond to 99% confidence intervals for the fitted parameters.

Catalyst	k_{cat} (min^{-1})	$K_{M\text{-}EDA}$ (mM)	$K_{M\text{-}styrene}$ (mM)	k_{cat} / $K_{M\text{-}EDA}$ (s^{-1} M^{-1})	k_{cat} / $K_{M\text{-}styrene}$ (s^{-1} M^{-1})	k_{cat} / ($K_{M\text{-}EDA}$ x $K_{M\text{-}styrene}$) (s^{-1} M^{-1} M^{-1})
P450$_{BM3\text{-}heme}$-CIS[2]	100 ± 24	5.2 ± 3.5	1.4 ± 0.5	320	1,100	2.1 x 10^5
P411$_{BM3\text{-}heme}$-CIS	82 ± 15	5.7 ± 2.9	4.6 ± 2.4	240	300	5.5 x 10^4

Nature Chemical Biology: doi:10.1038/nchembio.1278

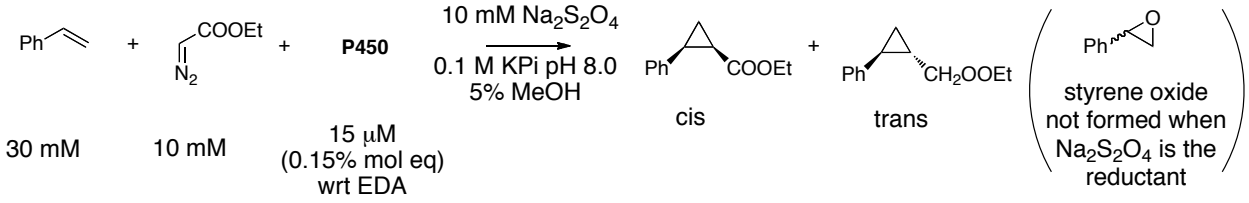

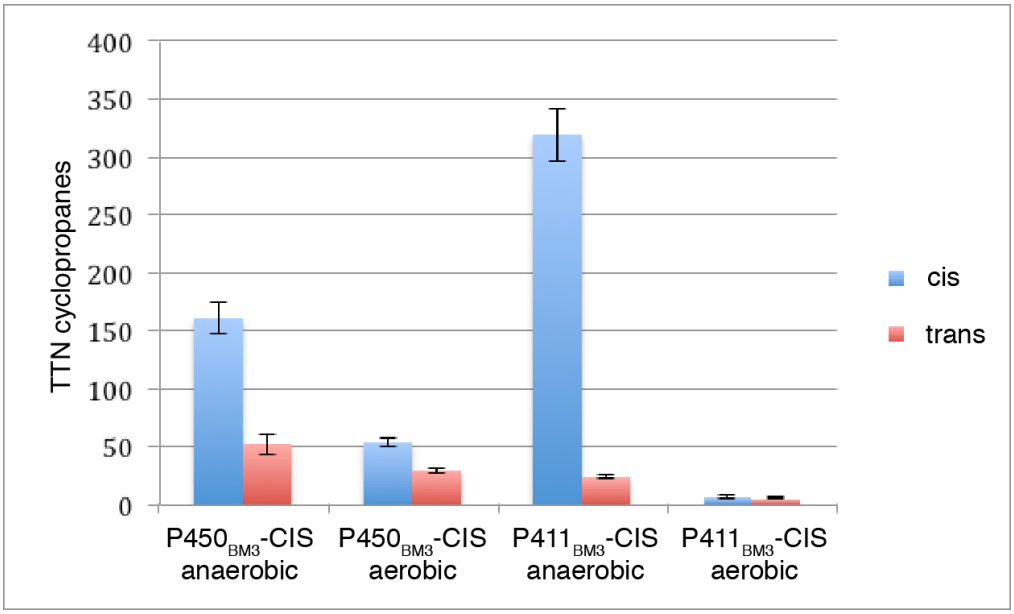

Supplementary Figure 11: Cyclopropanation activity under anaerobic *vs* aerobic conditions with dithionite in $P450_{BM3\text{-}heme}$-CIS and $P411_{BM3\text{-}heme}$-CIS. Measurements were taken in triplicate and the error bars represent the standard deviation of the measurements.

Supplementary Table 4: Activity under anaerobic *vs* aerobic conditions with dithionite in $P450_{BM3\text{-}heme}$-CIS and $P411_{BM3\text{-}heme}$-CIS.

Catalyst	Conditions	Yield (%)*	TTN	O_2 inhibition (%)	cis:trans[†]	%ee cis[‡]	%ee trans[§]
$P450_{BM3\text{-}heme}$-CIS	Anaerobic	32	212 ± 20	-	77:23	94	91
$P450_{BM3\text{-}heme}$-CIS	Aerobic	12	83 ± 5	-61	65:35	87	86
$P411_{BM3\text{-}heme}$-CIS	Anaerobic	51	342 ± 21	-	93:7	99	51
$P411_{BM3\text{-}heme}$-CIS	Aerobic	2	10 ± 1	-97	45:55	79	31

* Based on EDA. [†] Diastereomeric ratios and enantiomeric excess were determined by GC analysis. Major products: [‡]cis = (1*R*,2*S*) ; [§]trans = (1*S*,2*S*). Measurements were taken in triplicate and the error bars represent the standard deviation from the mean value.

Nature Chemical Biology: doi:10.1038/nchembio.1278

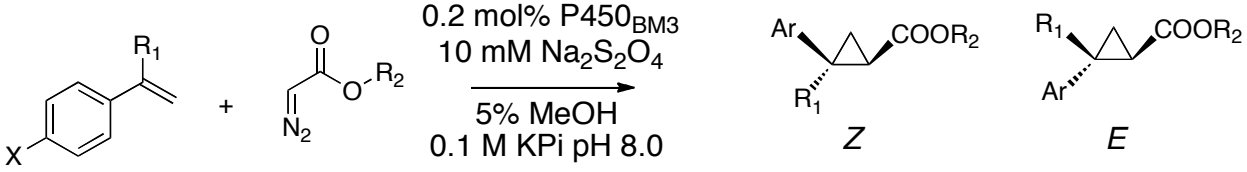

Supplementary Table 5: Enhanced *Z* selectivity for $P411_{BM3\text{-}heme}$-CIS over $P450_{BM3\text{-}heme}$-CIS.

Reagents	heme domain	% yield*	TTN	*Z*:*E*†	%ee *Z*‡	%ee *E*‡
R_1 = H, X = Me, R_2 = Et	$P450_{BM3}$-CIS	46	228	78:22	81.4	N/A
	$P411_{BM3}$-CIS	32	157	93:7	87.1	N/A
R_1 = H, X = OMe, R_2 = Et	$P450_{BM3}$-CIS	43	214	48:52	44	N/A
	$P411_{BM3}$-CIS	47	235	81:19	61	N/A
R_1 = H, X = CF_3, R_2 = Et	$P450_{BM3}$-CIS	42	211	39:61	54	93
	$P411_{BM3}$-CIS	24	121	76:24	55	75
R_1 = Me, X = H, R_2 = Et	$P450_{BM3}$-CIS	26	127	16:84	6	N/A
	$P411_{BM3}$-CIS	17	86	30:70	34	N/A
R_1 = H, X = H, R_2 = *t*-Bu	$P450_{BM3}$-CIS	0.3	2	3:97	N/A	N/A
	$P411_{BM3}$-CIS	15	76	8:92	N/A	N/A

* Based on EDA. † Diastereomeric ratios and enantiomeric excess were determined by GC analysis. ‡Enantiomeric excess is only reported when the enantiomers resolved to baseline resolution. GC methods for these products are reported in reference[2].

Nature Chemical Biology: doi:10.1038/nchembio.1278

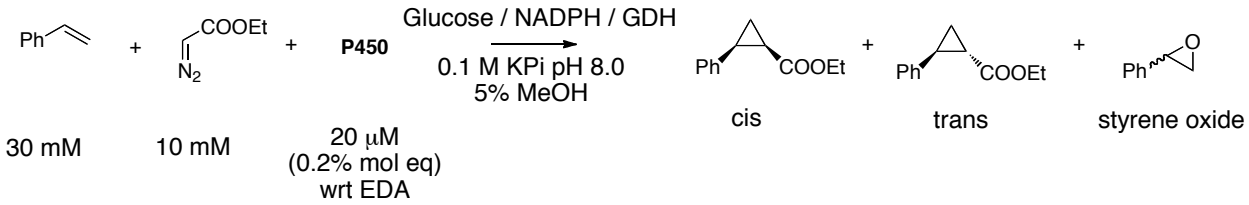

Supplementary Table 6:
In vitro activities for purified $P411_{BM3}$-CIS vs $P450_{BM3}$-CIS driven by NADPH.

Cat.	Conditions	Cyclopropanes (TTN_{cyc})	Styrene oxide (TTN_{epo})	TTN_{cyc} / TTN_{epo}	O_2 inhibition (%)	cis: trans*	%ee cis†	%ee trans‡
$P450_{BM3}$-CIS	Anaerobic	60 ± 18	12 ± 10	5	-	60 : 40	89	53
$P450_{BM3}$-CIS	Aerobic	82 ± 13	406 ± 21	0.20	+36	56 : 44	88	58
$P411_{BM3}$-CIS	Anaerobic	304 ± 15	0	-	-	72 : 28	92	19
$P411_{BM3}$-CIS	Aerobic	43 ± 5	14 ± 2	3.1	-86	49 : 51	74	14

* Diastereomeric ratios and enantiomeric excess were determined by GC analysis. Major products: †cis = (1*R*,2*S*) ;_‡trans = (1*S*,2*S*). Small-scale reactions (400 μL total volume) were conducted as described in the **Online Methods** with the following modifications: glucose dehydrogenase (GDH, 4 μL, 225 U mL^{-1}) was added to the reaction vial together with the P450 solution. Glucose (40 μL, 250 mM) and NADPH (40 μL, 5 mM) were degassed together with the buffer solution. Measurements were taken in triplicate and the error bars represent the standard deviation from the mean value. The small amounts of epoxide formed by $P450_{BM3}$-CIS under anaerobic conditions are due to dioxygen contamination in the small-scale reactions in our experiments.

Nature Chemical Biology: doi:10.1038/nchembio.1278

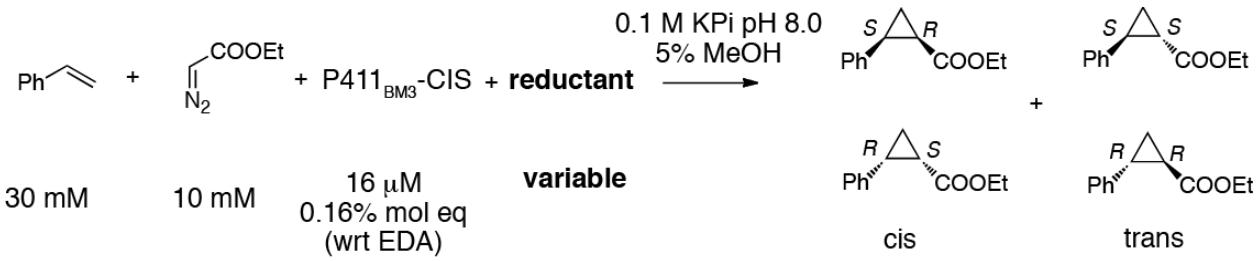

Supplementary Table 7:
In vitro $P411_{BM3}$-CIS cyclopropanation driven by $Na_2S_2O_4$, NADPH and NADH.

[NADPH] / mM	[NADH] / mM	[$Na_2S_2O_4$] / mM	Yield (%)*	TTN	cis:trans[†]	%ee cis[‡]	%ee trans[§]
0	0	0	1	3	54:46	-	-
0	0	10	35	218	94:6	99	43
1	0	0	47	294	93:7	98	40
5	0	0	58	364	90:10	97	28
10	0	0	49	305	91:9	98	26
0	1	0	70	437	93:7	98	38
0	5	0	68	428	93:7	98	34
0	10	0	47	295	93:7	98	34

* Based on EDA. [†] Diastereomeric ratios and enantiomeric excess were determined by GC analysis. Major products: [‡]cis = (1*R*,2*S*) ; [§]trans = (1*S*,2*S*).

Nature Chemical Biology: doi:10.1038/nchembio.1278

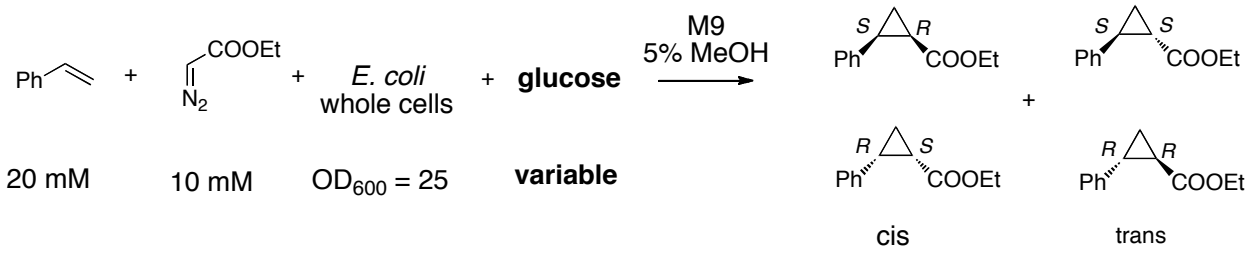

Supplementary Table 8: Effect of adding exogenous glucose (2 mM) on olefin cyclopropanation catalyzed by *E. coli* whole cells expressing $P450_{BM3}$-CIS or $P411_{BM3}$-CIS.

Whole-Cell Catalyst	[Glucose] (mM)	Yield (%)*	Total Turnovers (mmol g_{cdw}^{-1})	Effect of glucose addition (%)	Cell density (g_{cdw} L^{-1})	cis : trans[†]	%ee cis[‡]	%ee trans[§]
$P450_{BM3}$-CIS	0	7	0.12 ± 0.03	-	5.53	34 : 66	73	22
$P450_{BM3}$-CIS	2	13	0.24 ± 0.02	+98	5.53	48 : 52	86	30
$P411_{BM3}$-CIS	0	35	0.55 ± 0.06	-	6.38	70 : 30	95	11
$P411_{BM3}$-CIS	2	48	0.76 ± 0.01	+37	6.38	76 : 24	96	14

* Based on EDA. [†] Diastereomeric ratios and enantiomeric excess were determined by GC analysis. Major products: [‡]cis = (1*R*,2*S*) ; [§]trans = (1*S*,2*S*). Measurements were taken in triplicate and the error bars represent the standard deviation from the mean value. "Total turnovers" is defined as the amount of cyclopropane product (mmol) formed per mass of catalyst (g_{cdw}).

Nature Chemical Biology: doi:10.1038/nchembio.1278

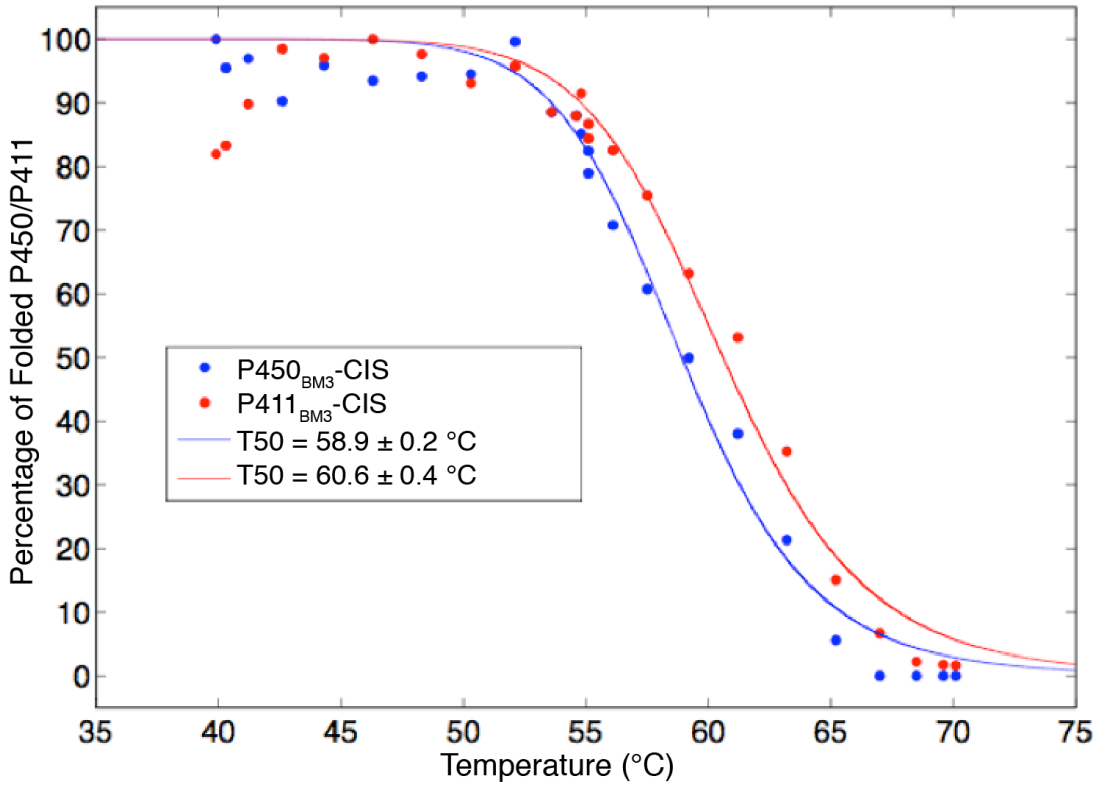

Supplementary Figure 12: Thermostabilities of $P450_{BM3}$-CIS (blue) and $P411_{BM3}$-CIS (red) heme domains. The C400S mutation stabilizes the heme domain by +1.7 °C. The T_{50} is the temperature at which half of the enzyme population has unfolded. Fitting error corresponds to 1-σ (68.3%) confidence intervals for the T_{50}.

Nature Chemical Biology: doi:10.1038/nchembio.1278

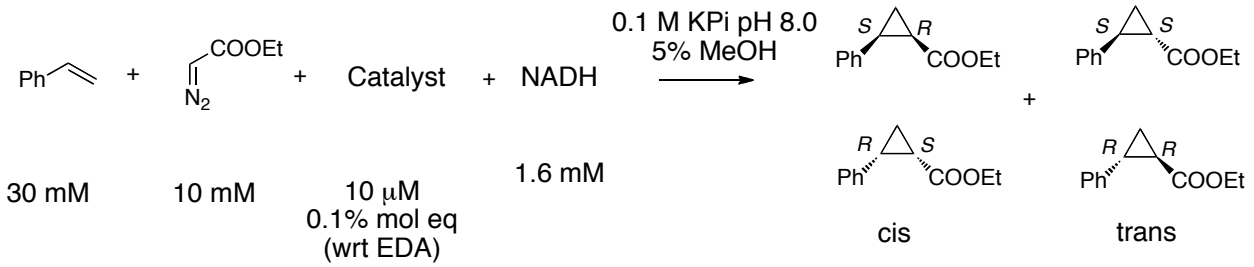

Supplementary Table 9:
In vitro cyclopropanation activities of $P450_{BM3}$ and $P411_{BM3}$ driven by NADH.

Catalyst	Yield (%)*	TTN	cis:trans[†]	%ee cis[‡]	%ee trans[§]
$P450_{BM3}$	0.2	2 ± 0.5	17:83	29	21
$P411_{BM3}$	36	364 ± 50	12:88	5	1

* Based on EDA. [†] Diastereomeric ratios and enantiomeric excess were determined by GC analysis. Major products: [‡]cis = (1*R*,2*S*) ;_[§]trans = (1*S*,2*S*). Small-scale (500 μL) reactions were conducted as described in the **Online Methods** with purified $P450_{BM3}$ and $P411_{BM3}$ catalysts. Measurements were taken in triplicate and the error bars represent the standard deviation from the mean value.

Nature Chemical Biology: doi:10.1038/nchembio.1278

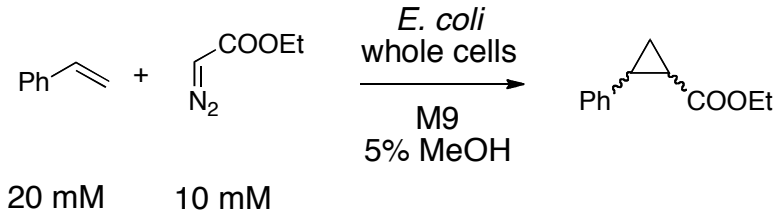

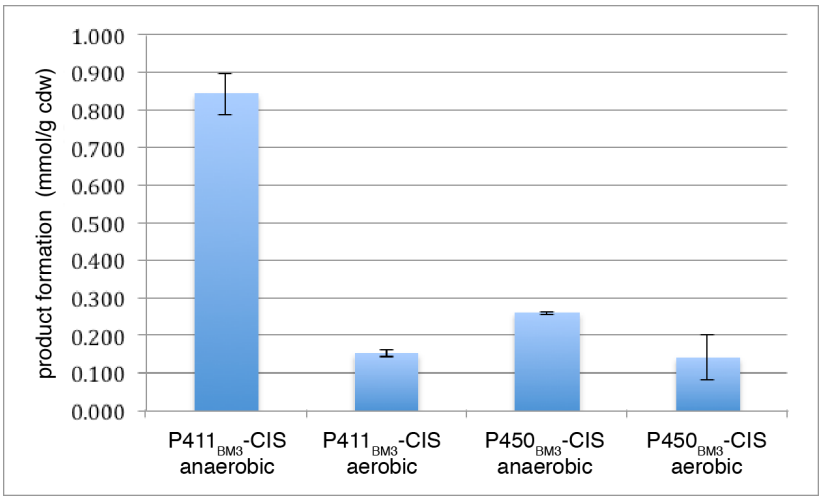

Supplementary Figure 13: Effect of dioxygen exposure on whole-cell catalyzed cyclopropanation. P411$_{BM3}$-CIS is strongly inhibited by dioxygen *in vivo*. All reactions had a cell density equivalent to OD_{600} = 25. Reactions were conducted in the absence of exogenous glucose. Measurements were taken in triplicate and the error bars represent the standard deviation from the mean value. Product formation is defined as the amount of cyclopropane product (mmol) formed per mass of catalyst (g_{cdw}).

Nature Chemical Biology: doi:10.1038/nchembio.1278

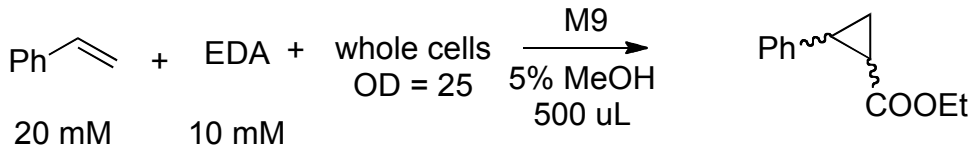

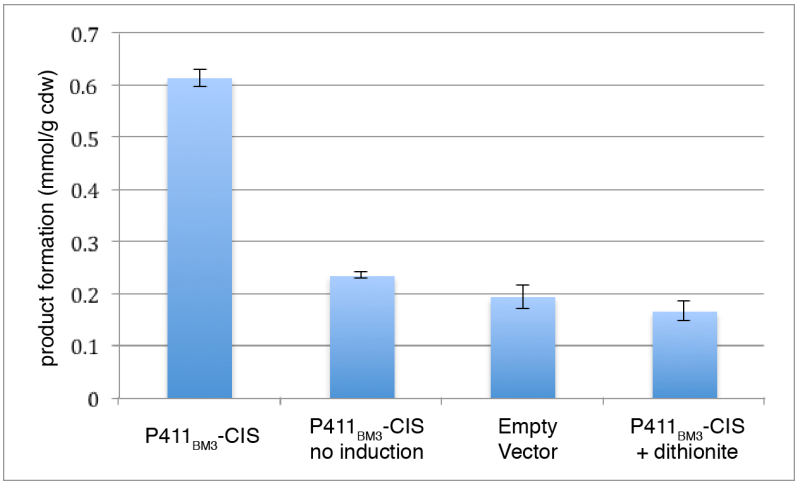

Supplementary Figure 14: Empty plasmid, no-induction controls and dithionite addition to whole cells. *E. coli* cells carrying the P411$_{BM3}$-CIS gene but grown without the addition of IPTG (P411$_{BM3}$-CIS no induction); *E. coli* cells carrying the pcWori plasmid but not the P411$_{BM3}$-CIS gene (empty pCWori); P411$_{BM3}$-CIS reaction with the addition of exogenous dithionite instead of glucose (ABC-CIS + dithionite). Reactions were left for two hours at 298 K. Measurements were taken in triplicate and the error bars represent the standard deviation from the mean value. Product formation is defined as the amount of cyclopropane product (mmol) formed per mass of catalyst (g_{cdw}).

Supplementary Table 10:
Empty plasmid, no induction controls and dithionite addition to whole cells.

Catalyst	Yield (%)*	cis:trans[†]	%ee cis[‡]	%ee trans[§]
P411$_{BM3}$-CIS	49	60:40	93	9
P411$_{BM3}$-CIS no induction	16	17:83	50	9
Empty pcWori	15	11:89	10	12
P411$_{BM3}$-CIS + dithionite	13	46:54	87	5

* Based on EDA. [†] Diastereomeric ratios and enantiomeric excess were determined by GC analysis. Major products: [‡]cis = (1*R*,2*S*) ; [§]trans = (1*S*,2*S*).

Nature Chemical Biology: doi:10.1038/nchembio.1278

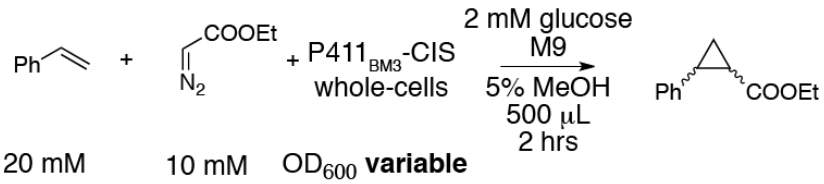

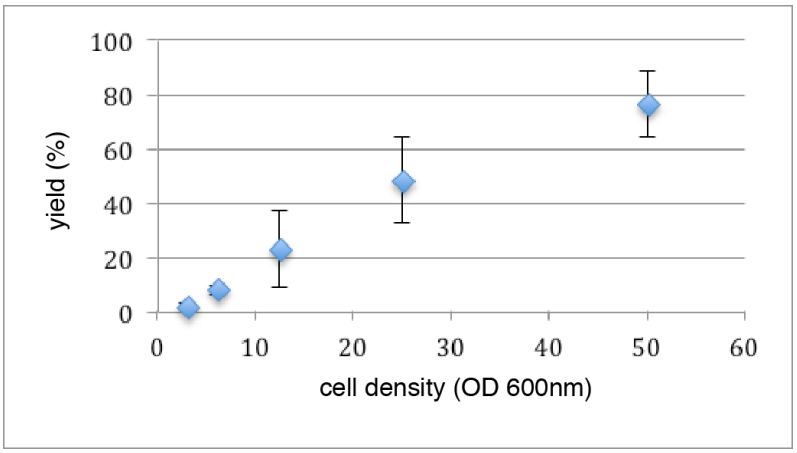

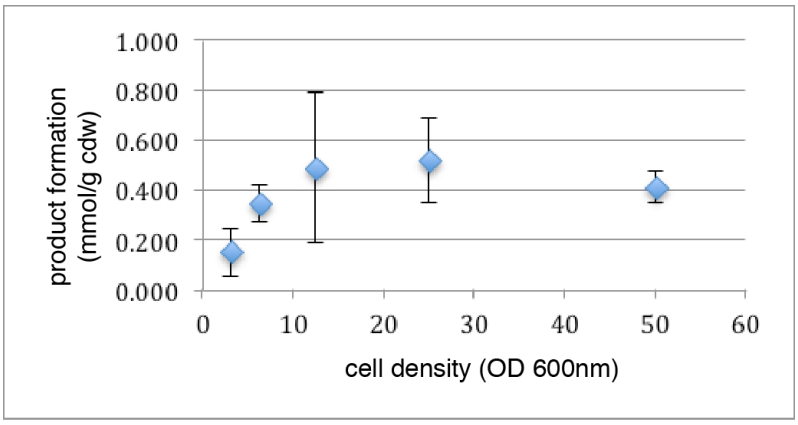

Supplementary Figure 15: Increasing cell density increases cyclopropane yields up ~80%. Total turnovers do not increase for cell densities higher than OD_{600} = 20. Measurements were taken in triplicate and the error bars represent the standard deviation from the mean value. Product formation is defined as the amount of cyclopropane product (mmol) formed per mass of catalyst (g_{cdw}).

Nature Chemical Biology: doi:10.1038/nchembio.1278

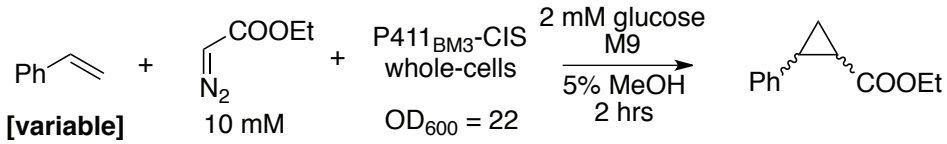

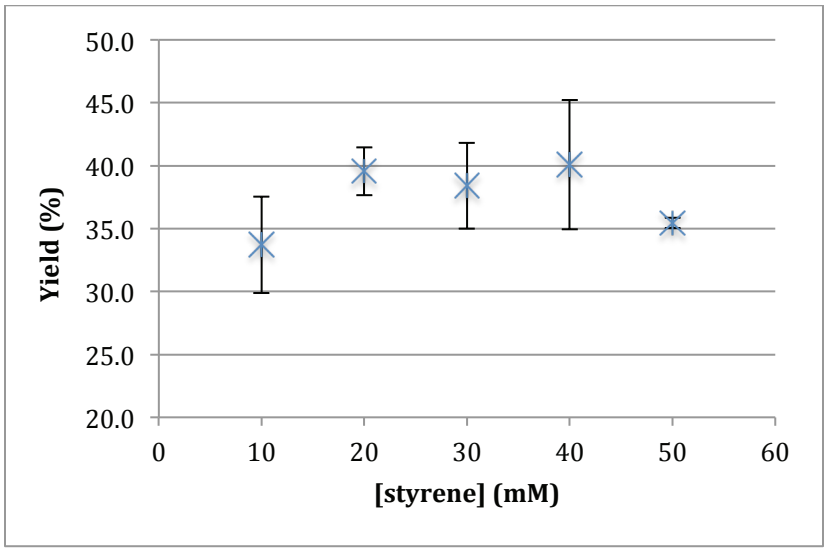

Supplementary Figure 16: Effect of using 1, 2, 3, 4 and 5 equivalents of styrene on reaction yield. Excess styrene gives only small improvements in yield. Measurements were taken in triplicate and the error bars represent the standard deviation from the mean value.

Nature Chemical Biology: doi:10.1038/nchembio.1278

Supplementary Table 11: Lysate activity compared to *in vivo* activity.

Catalyst	Conditions	[P411] (μM)	Yield (%)*	TTN	cis : trans[†]	%ee cis[‡]
$P411_{BM3}$-CIS	*In vivo*	1.0	44	5120	80:20	96
$P411_{BM3}$-CIS	Lysate, no reductant	1.0	0.6	55	67:33	92
$P411_{BM3}$-CIS	Lysate + NADH	1.0	18	1780	80:20	97
$P411_{BM3}$-CIS	Lysate + dithionite	1.0	0.8	79	64:36	86

* Based on EDA. [†] Diastereomeric ratios and enantiomeric excess were determined by GC analysis. Major products: [‡]cis = (1*R*,2*S*).

Nature Chemical Biology: doi:10.1038/nchembio.1278

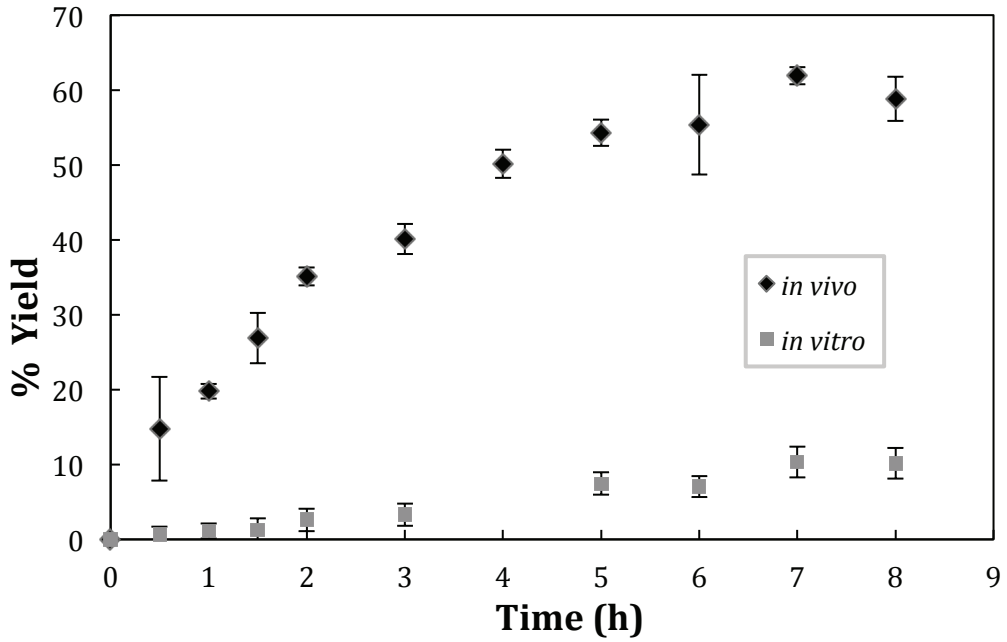

Supplementary Figure 17: Time course for *in vivo* and *in vitro* $P411_{BM3}$-CIS -catalyzed reaction at P411 loading of 1.6 μM [$\varepsilon_{411\text{-}490}$ = 103 mM^{-1} cm^{-1} for the ferrous-CO complex[1]]. Reaction conditions were as follows: 40 mM styrene, 20 mM EDA, 2 mM glucose, 10.2 g_{cdw} L^{-1} whole-cell $P411_{BM3}$-CIS (*in vivo*), 1.6 μM purified $P411_{BM3}$-CIS, 1 mM NADH (*in vitro*) in aqueous nitrogen-free M9 minimal medium and 5% MeOH cosolvent under anaerobic conditions at 298 K. Yields at each time point are reported as averages of two independent reactions.

Nature Chemical Biology: doi:10.1038/nchembio.1278

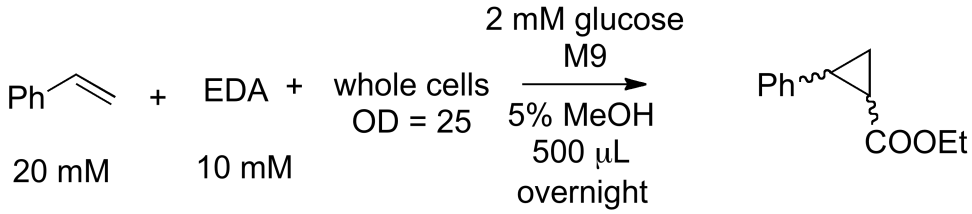

Supplementary Table 12:
Cyclopropanation activity of lyophilized $P411_{BM3}$-CIS whole-cell catalysts.

Catalyst	[Cell density] (g_{cdw} L^{-1})	[P411] (μM)	Yield (%)*	Total Turnover (mmol g_{cdw}^{-1})	TTN	cis : trans[†]	%ee cis[‡]	%ee trans[§]
$P411_{BM3}$-CIS	6.0	0.8	43	0.71 ± 0.08	5300 ± 600	67:33	93	25

* Based on EDA. [†] Diastereomeric ratios and enantiomeric excess were determined by GC analysis. Major products: [‡]cis = (1*R*,2*S*) ; [§]trans = (1*S*,2*S*). Cells were lyophilized in 10% sucrose (m/V) and were stored at 4 °C for two weeks. An appropriate mass of the resulting powder was transferred to a 2 mL glass vial, which was crimp sealed and purged with argon. Degassed solutions of nitrogen-free M9 medium and glucose (20 mM) were added via syringe. Cells were resuspended to OD_{600} = 25 and 2 mM final concentration of glucose. Measurements were taken in triplicate and the error bars represent the standard deviation from the mean value.

References

1 Vatsis, K. P., Peng, H.-M. & Coon, M. J. *J. Inorg. Biochem.* **91**, 542-553 (2002).

2 Coelho, P. S., Brustad, E. M., Kannan, A. & Arnold, F. H. *Science* **339**, 307-310 (2013).

Nature Chemical Biology: doi:10.1038/nchembio.1278